20% for D. For K they are less than 10%. For η, $(1/\tau - 1/\tau_0)$ is about $0.03\tau_{QP}^2/\tau_0^2$ times $(1/\tau - 1/\tau_0)$ for K. Thus, usually, the T^3 term in η will not be large, although it could be significant if τ_{QP}/τ_0 took on its extreme value of 3.1.

ACKNOWLEDGMENTS

I wish to thank D. Cheng for evaluating numerical integrals and for useful comments and discussion, and to acknowledge a free exchange of ideas with Dr. J. Sykes.

*Work supported by U. S. Atomic Energy Commission.
[1]V. J. Emery, Phys. Rev. 170, 205 (1968).
[2]G. Baym and C. Ebner, Phys. 170, 346 (1968)
[3]A. A. Abrikosov and I. M. Khalatnikov, Repts. Progr. Phys. 22, 329 (1959); D. Hone, Phys. Rev. 121, 669, 1864 (1961).
[4]M. J. Rice, Phys. Rev. 159, 153 (1967); *ibid.* 162, 189 (1967).
[5]V. J. Emery, Phys. Rev. 161, 194 (1967).
[6]W. R. Abel, R. T. Johnson, and J. C. Wheatley, Phys. Rev. Letters 18, 737 (1967).
[7]J. C. Wheatley, Phys. Rev. 165, 304 (1968).
[8]V. J. Emery and D. Cheng, Phys. Rev. Letters 21, 533 (1968).
[9]G. A. Brooker and J. Sykes, Phys. Rev. Letters 21, 279 (1968); H. Hojgard Jensen, H. Smith, and J. W. Wilkins, to be published.
[10]B. M. Abraham, Y. Eckstein, J. B. Ketterson, and J. H. Vignos, Phys. Rev. Letters 17, 1254 (1966).

PHYSICAL REVIEW VOLUME 175, NUMBER 1 5 NOVEMBER 1968

Large-Scale Self-Trapping of Optical Beams in the Paraxial Ray Approximation*

W. G. Wagner
University of Southern California, Los Angeles, California 90007, *and Hughes Research Laboratories, Malibu, California* 90265
and
H. A. Haus
Massachusetts Institute of Technology, Cambridge, Massachusetts
and
J. H. Marburger
University of Southern California, Los Angeles, California 90007
(Received 5 June 1968)

We present a systematic discussion of time-independent large-scale self-focusing in a paraxial ray "constant-shape" approximation. An equation is obtained for the variance of a self-focusing beam with a Gaussian transverse intensity profile as a function of axial distance. This equation, valid for an arbitrary nonlinear constitutive relation, is solved for several important situations, including the case of a saturable nonlinear refractive index. We also derive closed expressions for such a saturable index arising from reorientation of axially symmetric molecules in an external field, ignoring local-field effects. Self-focusing of an elliptically polarized beam is considered in the same approximation, and numerical results are presented which show that the self-focusing length is quite sensitive to small departures from circular polarization.

INTRODUCTION

In this paper we present a systematic discussion of time-independent self-trapping by molecular reorientation in a "paraxial ray" approximation. This approach provides a qualitative description of many of the important aspects of the stationary "large-scale" self-trapping phenomenon. In Sec. I, we review briefly some relevant previous work in order to place our own in proper context. Sec. II is an account of the approximation scheme used in this paper. We find that the equation describing the width of a propagating cylindrically symmetric beam (with an assumed Gaussian transverse intensity profile) is equivalent to the equation of motion of a particle in a one-dimensional conservative potential well. The potential is proportional to the nonlinear part of the dielectric susceptibility

describing the medium. Solutions of this equation are derived in Sec. III for susceptibilities which show nonsaturable and saturable behavior as a function of field strength. For an ideal liquid composed of molecules having uniaxial symmetry, we find a closed-form expression for the susceptibility arising from molecular reorientation which is "exact" if one ignores local field effects. This susceptibility displays the qualitative features of the simpler saturable model which is discussed in detail. In Sec. IV, we modify the preceding formalism to include polarization-dependent effects. There are now two coupled "equations of motion" describing the trapping of the right- and left-handed circularly polarized components of the light beam. These are solved numerically to find the critical power and self-trapping length for beams of arbitrary polarization.

I. OUTLINE OF PREVIOUS WORK

In many fluids the self-trapping of high-intensity light beams determines the onset of other nonlinear optical processes. The key role of this effect in such fluids has stimulated intensive research, both experimental and theoretical (see references below), into the details of the trapping mechanism. The experimental work has shown that the behavior of the beam is substantially different in two regimes. Initially a beam of the order of a millimeter or larger in transverse dimension contracts in a reasonably smooth way to a size of the order of 100 μ.[1] Typically at such sizes the contraction of the beam is sufficient to lead to field strengths which induce other important nonlinear processes, such as stimulated inelastic scattering of all types and double quantum absorption. At this stage, the beam begins to exhibit small-scale filamentation,[2–5] perhaps induced by fluctuations in the initial beam profile, with characteristic diameters of the order of 10 μ and less. These intense strands of light seem to last only about a nanosecond, probably as a result of large local thermal changes in the fluid which may cause small explosions, disrupting the beam. In these small-scale filaments, there is rapid and high conversion of the radiant energy from one frequency to another.

We refer to the regime where only the self-trapping phenomenon is important as the region of large-scale trapping. The subsequent behavior of the beam in the small-scale trapping regime is marvelously complex. Most efforts at a mathematical description of beam trapping, this paper included, have considered only beams with a fixed frequency, and are thus relevant only to propagation in the large-scale trapping regime. The interest in this work lies in the fact that good quantitative values for the threshold for inelastic nonlinearities may be obtained, and in the hope that some qualitative features of this description of beam propagation at very small transverse dimensions may appear in the small-scale trapping regime, where, however, the quantitative description may be quite different.

The theoretical treatments of self-trapping may be classified according to their goals and methods of analysis. Each has as its starting point Maxwell's equations and a nonlinear constitutive relation yielding an effective intensity-dependent refractive index. The resulting wave equation is then solved in varying degrees of approximation for the quantities of interest in the trapping situation. The first such quantity to be investigated was the critical power required in a beam for the focusing action to overcome diffraction defocusing. Solving the wave equation numerically, Chiao, Garmire, and Townes[6] found the critical power and the stationary radial intensity distribution for a beam having a single transverse intensity maximum. Critical powers for stationary beams having several maxima were found by Haus[7] using the same method. For beams which do not propagate with constant cross section, the spatial transition to a focus, characterized by a "self-focusing length" is of obvious importance. Using a form of the wave equation valid for regions in which the field amplitude changes slowly within a wavelength, Kelley[8] obtained a computer solution describing the field in a focusing (initially Gaussian) beam. Bespalov and Talanov[9] obtained numerical solutions of the same equation for beams with different initial shapes. All this work is valid only for linear polarization, and it employs the constitutive relation (for a real field)

$$\vec{D} = \epsilon_L \vec{E} + \epsilon_2 (\vec{E} \cdot \vec{E}) \vec{E} \tag{1.1}$$

which does not take saturation effects into account. Wagner and Reichert[10] have recently obtained critical powers and stationary radial intensity distributions for the "exact" susceptibility derived in Sec. III. C of this paper.

It is not necessary to resort to numerical computation to obtain useful formulas describing the most important aspects of trapping. Talanov,[11] Raizer,[12] and Akhmanov *et al.*[13] have used the approximate paraxial ray formalism of geometrical optics to find expressions for the critical power and the self-focusing length. We employ this formalism in the present paper, and discuss it in detail in Sec. II.

Bespalov and Talanov[9] have found useful information from a stability analysis of the wave equation with a cubic term. They assumed as an unperturbed solution a wave with no transverse intensity variation and asked for the growth rate of small perturbations. Perturbations with a transverse wavelength larger than a constant divided by the electric field strength were found to grow exponentially. If the maximum growth constant occurring in this type of analysis is regarded as the inverse of a characteristic trapping length, one finds trapping lengths *longer* than those given by other approaches for powers not exceeding the critical power by an order of magnitude. This is a consequence of the use of an unrealistically "flat" beam shape as the unperturbed solution. For powers much greater than the critical power, this analysis gives shorter trapping lengths, but only for an optimal Fourier component of the perturbation. Brueckner and Jorna[14] have also performed a stability analysis which attempts to encompass a wider variety of physical mechanisms.

Most of these techniques may be applied to more realistic self-trapping situations in which saturation

of the nonlinear index, polarization effects, time dependence, inelastic scattering, thermal effects, etc. are taken into account. In this paper, we analyze the time-independent saturation and polarization properties of trapping induced by molecular reorientation, ignoring all other complications. This is not unrealistic, since there are several liquids for which this effect is clearly the dominant self-trapping mechanism. It is also characterized by a shorter response time than other proposed mechanisms, and may therefore be analyzed independently of them in the spirit of an "adiabatic approximation." Finally, interaction with inelastically scattered waves is small in the large-scale trapping regime where the field intensity is still below threshold for stimulated processes.

II. THE PARAXIAL RAY APPROXIMATION

The electric and magnetic field intensities obey the equations

$$\nabla\times\vec{E} = -\mu\partial\vec{H}/\partial t \tag{2.1}$$

$$\nabla\times\vec{H} = \partial\vec{D}/\partial t \tag{2.2}$$

in rationalized mks units. These can be combined to give

$$\nabla\times(\nabla\times\vec{E}) + \mu\partial^2\vec{D}/\partial t^2 = 0, \tag{2.3}$$

where the displacement flux density is related to the electric field by a nonlinear constitutive law

$$\vec{D} = \overleftrightarrow{\epsilon}_L\cdot\vec{E} + \overleftrightarrow{\chi}(\vec{E})\cdot\vec{E}. \tag{2.4}$$

Here $\overleftrightarrow{\chi}$ is the nonlinear part of the susceptibility tensor the linear part being included in $\overleftrightarrow{\epsilon}_L$. In this section, we restrict the discussion to linearly polarized light and treat $\overleftrightarrow{\chi}$ as a scalar. In liquids, $\overleftrightarrow{\epsilon}_L$ may always be regarded as a scalar. Section IV includes the treatment for general polarization of $\vec{E}$.

When the dielectric constant varies with position, as when the nonlinear contribution to (2.4) is important, the electric field acquires a divergence and we have a vector problem. We shall disregard this effect, this obtaining from (2.3) the nonlinear scalar wave equation

$$\nabla^2E' + 2ik\partial E'/\partial z = -k^2\chi E'/\epsilon_L. \tag{2.5}$$

Here we have removed the rapidly varying part of the electric field strength

$$E = E'\exp[-i(\omega t - kz)],$$

where $k^2 = \epsilon_L\mu\omega^2$.

Complex notation in nonlinear equations must be handled with care. In the present situation, this problem is particularly simple because the only nonlinearity occurs in the susceptibility χ, which we assume to depend only on the field amplitude, and no frequency doubling, tripling, etc. is assumed to occur.

Equation (2.5) leads to the following equations for the slowly varying amplitude E_0 and phase ϕ of $E' = E_0\exp i\phi$, (∇_T is the gradient perpendicular to the direction of propagation and we assume cylindrical symmetry)

$$k\partial E_0^2/\partial z = -\nabla_T\cdot(E_0^2\nabla_T\phi), \tag{2.6}$$

$$2k\frac{\partial\phi}{\partial z} + (\nabla_T\phi)^2 - \frac{\nabla_T^2E_0}{E_0} - \frac{k^2}{\epsilon_L}\chi(E_0^2) = 0. \tag{2.7}$$

These are obtained from (2.5) by ignoring all second derivatives of ϕ and E_0 with respect to z and comparing real and imaginary parts. Equation (2.6) expresses the conservation of power, and (2.7) gives a differential equation for the surfaces of constant phase. The latter equation bears a striking resemblance to the Hamilton-Jacobi equation for a particle whose motion is described by the Hamiltonian $\frac{1}{2}p^2 + V$, $p = \nabla S$: $2\partial S/\partial t + (\nabla S)^2 + 2V = 0$. Identifying time with kz, spatial coordinates with kr, S with ϕ, and V with

$$-\frac{1}{2}\left(\frac{\nabla_T^2E_0}{k^2E_0} + \frac{1}{\epsilon_L}\chi\right) \equiv -\frac{1}{2}\frac{\epsilon_{\text{eff}}}{\epsilon_L}, \tag{2.8}$$

we find immediately from Hamilton's equations

$$d^2r/dz^2 = \tfrac{1}{2}(\partial/\partial r)(\epsilon_{\text{eff}}/\epsilon_L). \tag{2.9}$$

Here the position variable is the distance of a ray from the axis and depends upon the time variable z. Notice that the effective dielectric constant in (2.8) includes a term depending on the variation of field intensity across the wave front. This term describes the diffraction of the beam.

The right-hand side of (2.9) is a function of radius. This means that in order to evaluate the changes in shape of the light beam, it is necessary to trace a family of rays starting at different radial distances from the beam axis. Our next approximation, however, consists in replacing the right-hand side of (2.9) by a function proportional to the radial distance, thus vastly simplifying the mathematical effort. Before we can use (2.9), we must make the radial dependence of E_0 explicit. We assume that E_0 is given by

$$E_0 = E_m e^{-r^2/2a^2}, \tag{2.10}$$

where E_m and a^2 are functions of z. One reason for assuming this dependence is that it satisfies the equation of diffraction theory (the wave equation with $\partial^2E/\partial z^2$ neglected) in the absence of nonlinear effects.

Using Eq. (2.10), we find for the diffraction term in (2.8), at a radial distance $r = \alpha a$ with $\alpha \ll 1$,

$$\frac{1}{2k^2}\frac{\partial}{\partial r}\left(\frac{\nabla_T^2E_0}{E_0}\right)_{r=\alpha a} = \frac{1}{k^2}\frac{\alpha}{a^3}; \tag{2.11}$$

for a general nonlinear susceptibility $\chi(E_0)$, we find

$$\frac{1}{2\epsilon_L}\frac{\partial}{\partial r}[\chi(E_0)]_{r=\alpha a} \approx \frac{-1}{2\epsilon_L}\left(\frac{\partial\chi(E_0)}{\partial E_0}\right)_{r=\alpha a}\frac{\alpha E_m}{a}. \tag{2.12}$$

A relation between E_m and a can be obtained

from the expression for the power in the light beam, which quantity is conserved in the dissipation-free system we consider

$$P=\tfrac{1}{2}(\epsilon_L/\mu)^{1/2}\int_0^\infty E_m{}^2 e^{-r^2/a^2}2\pi r dr$$

$$=\tfrac{1}{2}\pi(\epsilon_L/\mu)^{1/2}E_m{}^2a^2. \qquad (2.13)$$

In evaluating the power, we have neglected the change in dielectric constant with applied electric field. Here E_m is the peak amplitude and the power is averaged over one cycle. To obtain the corresponding result in unrationalized cgs units, divide (2.13) by $4\pi\epsilon_0$.

Now (2.12) may be written as a function of a alone

$$\frac{1}{2\epsilon_L}\frac{\partial}{\partial r}\chi(E_0)\Big|_{r=\alpha a}\approx-\frac{1}{2\epsilon_L}\frac{\partial\chi(E_0)}{\partial E_0}\Big|_{r=\alpha a}\frac{q\alpha}{a^2},$$

where $q^2=(2/\pi)(\mu/\epsilon_L)^{1/2}P$. (2.14)

Equation (2.9) may now be written as an ordinary differential equation for the beam radius a

$$\frac{\partial^2 a}{\partial z^2}=\frac{1}{k^2a^3}-\frac{q}{2\epsilon_L a^2}\frac{\partial\chi(E_0)}{\partial E_0}\Big|_{r=\alpha a}. \qquad (2.15)$$

This may be rewritten in the following suggestive form:

$$\partial^2 a/\partial z^2=-\partial U/\partial a, \qquad (2.16)$$

$$U(a)=(2k^2a^2)^{-1}-(2\epsilon_L)^{-1}\chi(q/a). \qquad (2.17)$$

Equation (2.16) is equivalent to that describing a particle of unit mass moving in the one-dimensional conservative potential U. Thus, once the nonlinear susceptibility is specified, we may use the formal apparatus of elementary mechanics to find the behavior of the beam radius a as a function of z. In particular, the minimum beam radius a_m, if any, may be found using "conservation of energy"

$$U(a_m)=U(a_0)+\tfrac{1}{2}\dot{a}_0{}^2 \qquad (2.18)$$

Here a_0 is the initial beam size and $\dot{a}_0=\tan\theta_0$, where θ_0 is the initial divergence angle of the beam. Once a_m has been found, the distance z_f from $z=0$, at which this minimum occurs, is given by the familiar formula for the "half period" of the motion

$$z_f=\int_{a_0}^{a_m}da/\{2[U(a_0)-U(a)]+\dot{a}_0{}^2\}^{1/2}. \qquad (2.19)$$

A beam with no initial divergence and with size a_c given by the solution of (2.15), with $\partial^2 a/\partial z^2=0$, will propagate with constant cross section. Evidently the expression

$$(k^2a_c q/2\epsilon_L)[\partial\chi(E_0)/\partial E_0]\Big|_{r=\alpha a_c}=1, \qquad (2.20)$$

is an implicit equation for a_c. This corresponds to the value of a for which the slope of U vanishes, a point of "equilibrium."

In the next section we consider some applications of this formalism for particular susceptibilities.

III. NONLINEAR SUSCEPTIBILITIES

A. Simplest Nonsaturable Susceptibility

Expanding the nonlinear part of the susceptibility and keeping only the first nonvanishing term, we find for an isotropic medium

$$\chi_0(E_0)\approx\epsilon_2' E_0{}^2, \qquad (3.1)$$

where our notation for the coefficient of proportionality conforms with Kelley's.[8] While this form does not include saturation, it is the simplest which leads to self-trapping when ϵ_2' is positive. The effective potential corresponding to (3.1) is

$$U_0=(2a^2k^2)^{-1}[1-(\epsilon_2'/\epsilon_L)k^2q^2], \qquad (3.2)$$

which is "attractive" (leads to focusing solutions) only for

$$q^2\geq\frac{\epsilon_L}{\epsilon_2'k^2}\quad\text{or}\quad P\geq P_{cr}\equiv\frac{\pi\epsilon_L{}^{3/2}}{2\epsilon_2'k^2\mu^{1/2}}, \qquad (3.3)$$

where P_{cr} is the critical power for focusing. This critical power is less than that found numerically by Chiao, Garmire, and Townes,[6] by the factor $\pi/(2\times5.763)=0.273$.

Equation (2.16) may be solved directly in this case for a formula which describes most of the important aspects of the self-trapping phenomenon

$$\frac{a^2}{a_0{}^2}=\left(1-\frac{P}{P_{cr}}\right)\frac{z^2}{k^2a_0{}^4}+(1+\dot{a}_0\frac{z}{a_0})^2. \qquad (3.4)$$

This solution is plotted in Fig. 1 for $P=10P_{cr}$. The dimensionless variables employed in the figure are $\eta^*=a/a_0$, $\zeta^*=z/ka_0{}^2$, and $\theta_0=\tan^{-1}[(P/P_{cr}-1)/a_0k]$. When the divergence angle of the incident beam is greater than θ_0, there is no focus for positive values of z. For an initial beam diameter of 0.2 cm and light at 6900 Å, this angle is close to a milliradian at $P=10P_{cr}$. Figure 1 indicates that the self-focusing length is a sensitive function of the incident divergence.

The equilibrium radius defined by (2.20) exists only when $\dot{a}_0=0$, $P=P_{cr}$; under these conditions it is arbitrary. Thus a beam of any size and no initial divergence will propagate with constant cross section if it has precisely the critical power. This is true only for the approximate susceptibility (3.1). For saturable susceptibilities, there is usually a unique critical radius for each power exceeding the critical power.

For P sufficiently large, the beam collapses to an arbitrarily small radius at a distance z_f given by

$$\frac{z_f}{a_0}=\frac{ka_0}{(P/P_{cr}-1)^{1/2}-a_0\dot{a}_0k}. \qquad (3.5)$$

Evidently the power in a divergent beam must exceed

$$P_{max}=[1+(a_0\dot{a}_0k)^2]P_{cr} \qquad (3.6)$$

before it can trap itself. Raizer,[12] however, has

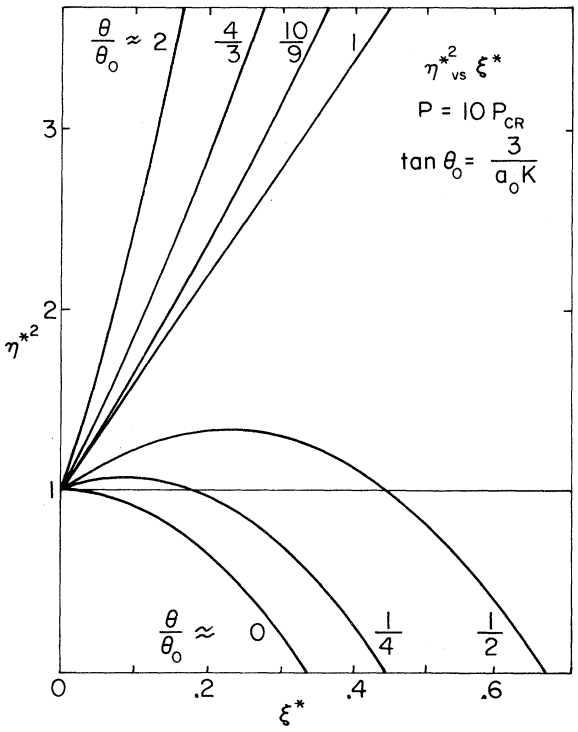

FIG. 1. Radius squared versus axial distance in dimensionless variables for various divergence angles of the incident beam in the absence of saturation for $P=10P_{\cdot}$. $\xi^*=z/Ka_0^2$, $\eta^*=a/a_0$.

pointed out that *part* of a divergent beam can become trapped at powers lower than this.

To estimate the critical power required to trap any part of a beam, Raizer assumes an equation equivalent to (3.6) to apply to a tube within the beam characterized by $a_{01}\leq a_0$ and $\mathring{a}_{01}$ proportional to a_{01}. However this assumption implies that the trapping of each tube within the main beam is governed by a different transverse intensity distribution. This is certainly inconsistent with other assumptions used in deriving (3.6).

Equation (3.4) may be used to compute the intensity on the z axis. Taking $I=P/\pi a^2$, we find

$$\frac{I}{I_0}=[(1-\frac{P}{P_{cr}})\frac{z^2}{k^2a_0^4}+(1+\mathring{a}_0\frac{z}{a_0})^2]^{-1}. \quad (3.7)$$

This differs from the empirical expression given by Kelley[8] even for parallel incident beams. Kelley's formula leads to imaginary intensities for $P<P_{cr}$ and is therefore not useful for investigations of trapping near threshold. Kaiser *et al.*[15] explain why Kelley's equation is accurate in some cases despite its awkward analytical properties, and modify it to include absorption. An analogous modification of (3.7) is possible, but is not relevant to our discussion.

B. Simplest Saturable Susceptibility

Replacing ϵ_2' in (3.1) with the "standard" saturable form

$$\epsilon_2'=\epsilon_{20}'[1+(E_0^2/E_s^2)]^{-1}, \quad (3.8)$$

we obtain an expression for the susceptibility which displays most of the qualitative aspects of the "exact" form to be derived below. The principal new features are a minimum radius for the focused beam and "pulsations" or repeated foci as noted by Razier.[12] All other aspects of the nonsaturable case appear here as well, but we confine the discussion to parallel incident beams for brevity.

The "equation of motion" of the radius is now

$$k^2\frac{d^2a}{dz^2}=\frac{1}{a^3}\left(1-\frac{P/P_{cr}}{[1+(a_s^2/a^2)]^2}\right), \quad (3.9)$$

where $a_s=q/E_s$. (3.10)

Figure 2 shows a graph of the corresponding potential

$$k^2U_s=\frac{1}{2a^2}\left(1-\frac{P/P_{cr}}{1+(a_s^2/a^2)}\right), \quad (3.11)$$

which reduces to (3.2) for large values of the saturation field E_s. The dimensionless variables employed in this and subsequent figures are

$$\eta=a/a_s, \quad \xi=z/ka_s^2.$$

Here a_s is the radius to which a beam of definite power must shrink before saturation effects become appreciable. In terms of the physical model for saturation described in the next section, we have

$$E_s=(4kT/|\alpha_{\parallel}-\alpha_{\perp}|)^{1/2}.$$

At this field strength, the energy associated with the reorientation of an induced molecular dipole is kT. A glance at Fig. 6, in which saturable susceptibilities are plotted versus $E^2/E_s^2=a_s^2/a^2=\xi^2$, shows that the dielectric response of the medium actually flattens out only for $a\lesssim a_s/3$. For CS_2 at room temperature, $a_s=3.12\sqrt{P}\,\mu$ for P in megawatts. (This number does not include local field corrections.) The quantity actually

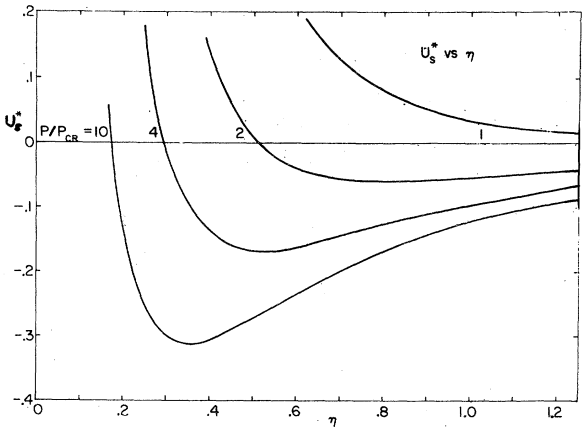

FIG. 2. Effective potential versus beam radius for the saturable susceptibility of Eq. (3.1). $\eta=a/a_s$.

plotted in Fig. 2 is $U_S^* \equiv (4\epsilon_L V/N|\alpha_\parallel - \alpha_\perp|)U_S$, where N/V is the molecular number density and $\alpha_\parallel$ and $\alpha_\perp$ are the longitudinal and transverse polarizabilities of the axially symmetric molecules of our model.

The equilibrium radius given by (3.9) is

$$a_c = a_S[(P/P_{cr})^{1/2} - 1]^{-1/2} . \quad (3.12)$$

For powers greatly exceeding the trapping threshold value P_{cr}, the equilibrium radius is proportional to $P^{1/4}$. This may be surprising at first glance because the dielectric constant reaches a power-independent saturation value at high P. However, a look at (2.20) shows that the gradient of χ, and not χ itself, determines the equilibrium radius. Order-of-magnitude estimates of a_c are are given in Sec. III. C. For the present, we remark that for $P = P_S \gg P_{cr}$, where $P_S \equiv P/k^2 a_S^2$,

$$k^2 a_c^2 \approx \left(\frac{P_{cr}}{P_S}\right)^{1/2} = \left(\frac{\epsilon_L}{\epsilon_{20} E_S^2}\right)^{1/2} = \left(\frac{\epsilon_L}{\delta\epsilon}\right)^{1/2} ,$$

where $\delta\epsilon$ is the maximum change in the dielectric constant achieved at full saturation. $a_c \gg \lambda$ only if the maximum fractional change in the dielectric constant is much smaller than unity. Since the radius oscillates weakly about the equilibrium point a_c in this model, we know that the minimum radius reached will always be less than a_c. Thus a self-focusing beam will tend to focus to radii less than a wavelength unless $\delta\epsilon \ll 1$ or $P \approx P_{cr}$. Of course, our analysis fails for such small radii because the neglect of second derivatives with respect to z is no longer justified, and the details of propagation will be modified substantially in the focal region by other nonlinear phenomena.

When the radius of the light beam oscillates weakly about its equilibrium position, the "period" or interval between minimum radii (foci) may be obtained from a "small-signal" analysis of (3.9). In this approximation, the squared angular frequency is equal to the spring constant

$$k^2\omega^2 = -\frac{d}{da}\frac{1}{a^3}\left(1 - \frac{P/P_{cr}}{[1 + (a_S^2/a^2)]^2}\right)_{a=a_0} , \quad (3.13)$$

from which the period is found to be

$$z_S = 2\pi\omega^{-1} = \pi k a_S^2 \frac{(P/P_{cr})^{1/4}}{[(P/P_{cr})^{1/2} - 1]^{3/2}} . \quad (3.14)$$

For $P \approx P_{cr}$, or when the saturation field is very small, z_f is much greater than the near field length ka_S^2 of a beam of radius a_S.

The period for large oscillations can be found from the exact solution of Eq. (3.9). For a parallel incident beam, we have

$$\xi = \frac{1}{2}\int_{\eta_0^2}^{\eta^2} \frac{(X+1)^{1/2} dX}{\{[(P/P_{cr}) - 1]X - 1 - CX(X+1)\}^{1/2}} , \quad (3.15)$$

where $C \equiv \{[(P/P_{cr}) - 1]\eta_0^2 - 1\}/\eta_0 + 1)\eta_0^2$. (3.16)

This can be written as an incomplete elliptic integral of the second kind

$$z = \frac{P}{kP_S}\frac{(\eta_0^2 + 1)}{[(P/P_{cr}) - 1 - \eta_0^{-2}]^{1/2}} E(\Phi, \gamma) , \quad (3.17)$$

where

$$\sin^2\Phi = \frac{\eta_0^2 - \eta^2}{\eta_0^2 - \eta_m^2} ,$$

$$\gamma^2 = \frac{[(P/P_{cr}) - 1]\eta_0^4 - 2\eta_0^2 - 1}{(\eta_0^2 + 1)\{[(P/P_{cr}) - 1]\eta_0^2 - 1\}} . \quad (3.18)$$

Here $\eta_m a_S$ is the minimum radius a_m which can be found from (2.18) or from the condition that the integrand of (3.15) be singular at η_0^2 and η_m^2. When $\dot{a}_0 = 0$, we have

$$\eta_m^2 = (\eta_0^2 + 1)/\{[(P/P_{cr}) - 1]\eta_0^2 - 1\} .$$

The exact "half period" or self-focusing length is

$$\frac{z_f}{ka_S^2} \equiv \xi_f = \frac{(\eta_0^2 + 1)}{[(P/P_{cr}) - 1 - \eta_0^{-2}]^{1/2}} E(\gamma) , \quad (3.19)$$

where $E(\gamma)$ is the complete elliptic integral of the second kind. Our notation for these integrals is that of Abramowitz and Stegun.[16]

Figure 3 shows the dimensionless minimum radius η_m as a function of starting radius η_0, and Fig. 4 gives the dimensionless period of oscillation as a function of starting radius with P/P_{cr} as parameter. Neither of these quantities are sensitive functions of a_0 for large starting radii

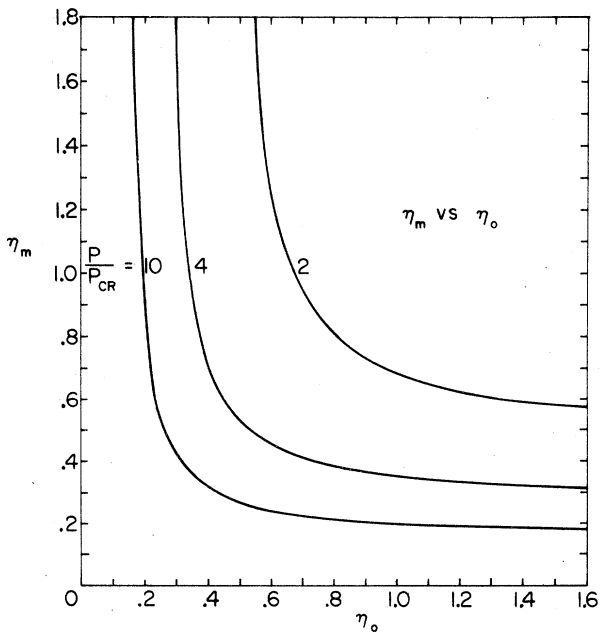

FIG. 3. Minimum (or maximum) radius versus starting radius. $\eta = a/a_S$.

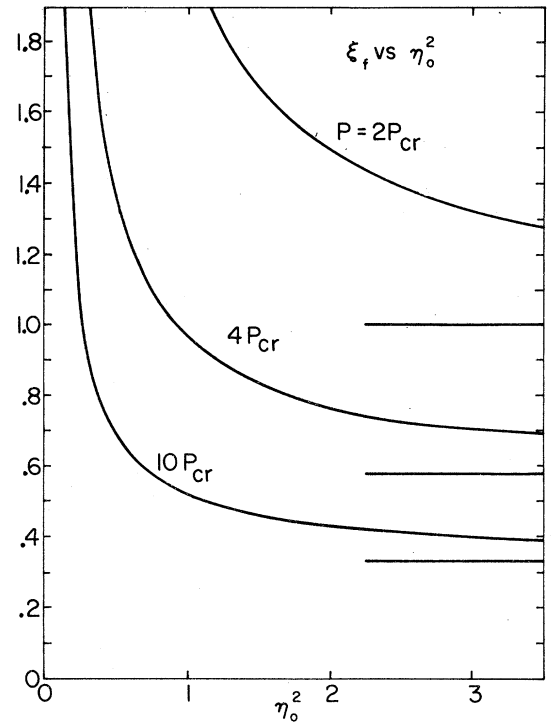

FIG. 4. Self-trapping length versus radius of incident beam. Asymptotes are indicated for $\eta_0 = a_0/a_S \rangle\rangle 1$. $\xi_f = z_f/Ka_S^2$.

$a_0 \gg a_S$. Figure 5 shows trajectories for a given P/P_{cr} with three different starting radii. The distance between foci is twice zf, which measures the distance of the first focus from $z = 0$ for a parallel incident beam. For larger starting radii, the first minimum falls close to $\xi_f = \frac{1}{3}$ for this case, i.e., to $(P/P_{cr} - 1)^{-1/2}$.

C. Susceptibility Corresponding to Molecular Reorientation

In this section, we compute the susceptibility of a model liquid consisting of N noninteracting molecules with uniaxial symmetry in a volume V, ignoring local field effects. The energy of one such molecule in the presence of an external electric field inclined at angles θ, φ with respect to the principal axis system is

$$w(\theta, \varphi) = -\tfrac{1}{2} \sum_{ij} \alpha_{ij}(\theta, \varphi) \langle E_i E_j \rangle_t \ . \qquad (3.20)$$

Here the $\langle\!\langle \ \rangle\!\rangle_t$ indicates a time average over many cycles of the field, and α_{ij} (θ, φ) is the polarizability tensor obtained by a transformation from the molecular principal axis system

$$\alpha_{ij}(\theta, \varphi) = \sum_{kl} A_{ik}(\theta, \varphi) A_{jl}(\theta, \varphi) \alpha_{kl}^{\,0} \qquad (3.21)$$

where, for uniaxial symmetry,

$$(\alpha_{ij}^{\,0}) = \begin{pmatrix} \alpha_\perp & 0 & 0 \\ 0 & \alpha_\perp & 0 \\ 0 & 0 & \alpha_\parallel \end{pmatrix} .$$

The rotation matrix A_{ij} (θ, φ) is that given by Goldstein.[17] (Rotation through ψ about the body axis leaves our system unchanged, so we take $\psi = 0$.) In a liquid, the presence of surrounding molecules modifies the field seen at any point. However, the nonlinear local field problem for this case is sufficiently difficult to warrant a separate investigation, and we neglect it completely in the following discussion.

For $\langle E \rangle_t$ linearly polarized in the x direction, we may write the partition function describing an ensemble of molecules, each with energy given by (3.21), as

$$Z = \tfrac{1}{2} \int_{-1}^{1} \exp\{\tfrac{1}{4}\beta E_0^{\,2}[\alpha_\perp + (\alpha_\parallel - \alpha_\perp)\cos^2\theta]\} d\cos\theta \ , \qquad (3.22)$$

the φ integration being trivial for our symmetry. Here $\beta = (k_B T)^{-1}$ and θ is the angle between the symmetry axis and the direction of polarization. E_0 is the *peak* electric field intensity.

The integral in (3.22) may be evaluated explicitly, and has different forms depending upon the sign of $(\alpha_\parallel - \alpha_\perp)$. For "cigar-shaped" molecules such as CS_2, $(\alpha_\parallel - \alpha_\perp) > 0$, and we have

$$Z_+ = (E_S/E_0) e^{\frac{1}{4}\beta\alpha_\parallel E_0^{\,2}} F(E_0/E_S) \ , \qquad (3.23)$$

where $F(x)$ is Dawson's integral (tabulated in Ref. 16)

$$F(x) \equiv e^{-x^2} \int_0^x e^{y^2} dy$$

and $E_S = 2(\beta|\alpha_\parallel - \alpha_\perp|)^{-1/2}$.

For disc-shaped molecules such as benzene, $\alpha_\parallel - \alpha_\perp < 0$ and

$$Z_- = \tfrac{1}{2}\pi^{\frac{1}{2}} (E_S/E_0) e^{\frac{1}{4}\beta\alpha_\perp E_0^{\,2}} \operatorname{erf}(E_0/E_S) \ , \qquad (3.24)$$

where the error function $\operatorname{erf}(x) \equiv (2/\pi^{1/2}) \int_0^x e^{-y^2} dy$ is also tabulated in Ref. 16.

These formulas lead directly to expressions for the mean polarizability, and therefore to the polar-

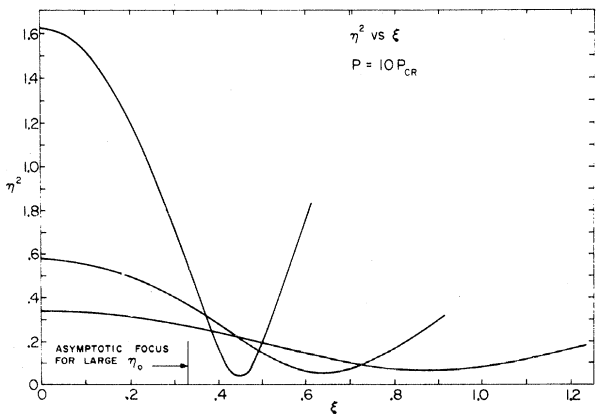

FIG. 5. Radius squared versus axial distance for different starting radii. The curves are all periodic, with period twice the distance to the first minimum.

ization density and a constitutive relation as well. For the mean polarizability, we have

$$\bar{\alpha}_{\pm} = (4/\beta)\partial \ln Z_{\pm}/\partial(E_0^2)$$
$$= \alpha + \tfrac{1}{2}|\alpha_{\parallel} - \alpha_{\perp}|\left(\mp\frac{2}{3} - \frac{1}{\zeta^2} + \frac{1}{\zeta G_{\pm}(\zeta)}\right), \quad (3.25)$$

where, taking $\zeta = E_0/E_S = \eta^{-1}$,

$$G_{+}(\zeta) \equiv F(\zeta), \quad G_{-}(\zeta) \equiv (\sqrt{\pi}/2)e^{\zeta^2}\,\mathrm{erf}(\zeta),$$
$$\alpha \equiv \tfrac{1}{3}(\alpha_{\parallel} + 2\alpha_{\perp}).$$

The bracketed expression in (3.25) vanishes at zero field, so the linear dielectric constant and nonlinear susceptibility are, respectively,

$$\epsilon_L = \epsilon_0 + (N/V)\alpha$$

and

$$\chi_{\pm}(E) = \frac{N|\alpha_{\parallel} - \alpha_{\perp}|}{2V}\left(\mp\frac{2}{3} - \frac{1}{\zeta^2} + \frac{1}{\zeta G_{\pm}(\zeta)}\right). \quad (3.26)$$

The dimensionless susceptibilities $\Xi_{\pm} = [2V/(N|\alpha_{\parallel} - \alpha_{\perp}|)]\chi_{\pm}$ are shown in Fig. 6 as functions of ζ. For comparison, we have also plotted the dimensionless simple saturable susceptibility Ξ_S corresponding to (3.8) and (3.1). The saturation field E_S has been chosen to give the same saturated susceptibility as that of Ξ_-. The saturation values of χ_+ and χ_- are different because when added to the linear part of susceptibility $(N/V)\frac{1}{3}(\alpha_{\parallel} + 2\alpha_{\perp})$ they must give $(N/V)\alpha_{\parallel}$ and $(N/V)\alpha_{\perp}$, respectively.

Figure 7 shows these susceptibilities on an expanded scale for small dimensionless field strengths ζ. To fourth order in ζ, we have

$$\Xi_{\pm}(\zeta) \approx \frac{8}{45}\zeta^2 \pm \frac{16}{945}\zeta^4, \quad (3.27)$$

$$\Xi_S(\zeta) \approx \frac{8}{45}\zeta^2 - \frac{32}{675}\zeta^4. \quad (3.28)$$

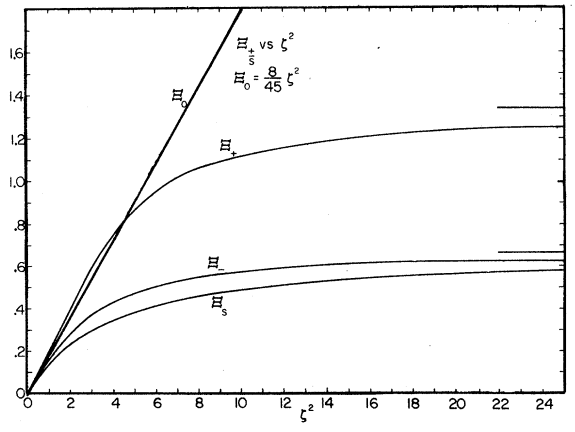

FIG. 6. Dimensionless susceptibilities $\Xi_{\pm}$ for prolate and oblate molecules, respectively, Ξ_S for the standard saturable form Eq. (3.1), and the nonsaturable form Ξ_0, all versus $\zeta^2 = E^2/E_S^2 = a_S^2/a^2$.

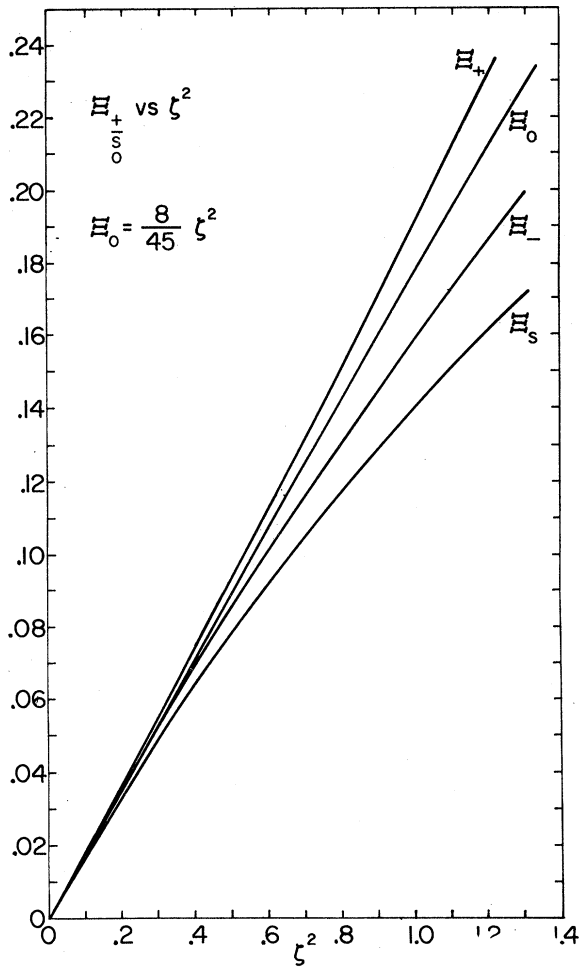

FIG. 7. Expanded view of Fig. 6 for small intensities.

It is interesting that for cigar-shaped molecules the susceptibility shows positive curvature as a function of intensity before saturation begins to be significant. However, a glance at Fig. 8 shows that the potentials arising from all three susceptibilities are very much the same. Thus most qualitative aspects of self-trapping are described adequately by the simple model of the previous section, for which explicit solutions have been obtained. However Chiao *et al.*[18] and also Reichert and Wagner[10] have shown that for χ_+ there are *two* equilibrium radii for some input beam powers. Numerical solution of an equation similar to that given by Chiao, Garmire, and Townes,[6] but including χ_+ and crude local-field corrections, gives two stationary transverse intensity distributions of width 1.8 and 0.4 μ for CS_2 and $\lambda = 0.69\,\mu$. The power in each beam is about 7.5 kW, the critical power in this analysis being about 7 kW.[10] Neither of these distributions has nodes for finite radii.

The dimensionless potentials U^* in Figs. 2 and 8 are defined through

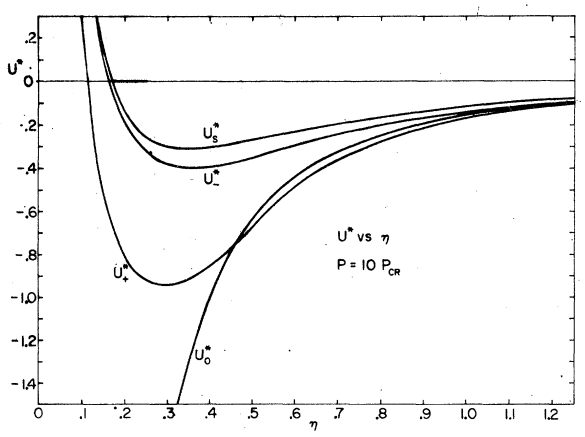

FIG. 8. Dimensionless potentials corresponding to the susceptibilities shown in Fig. 6 plotted versus $\eta = a/a_S$.

$$U^* \equiv \frac{4\epsilon_L}{(N/V)|\alpha_\parallel - \alpha_\perp|} U \ ,$$

$$\text{or} \quad U^* = \frac{8}{45}(P_{cr}/P)\xi^2 - \Xi(\xi^2) \ .$$

In the high- and low-field limits, the local field problem becomes tractable for our ideal fluid, and we may find the maximum fractional change in dielectric constant from the Lorentz local field theory.

$$\frac{\delta\epsilon}{\epsilon_L} = \frac{1}{\epsilon_L}\frac{N}{V}\left(\frac{\alpha_m}{1-\frac{1}{3}(N/V)\alpha_m/\epsilon_0} - \frac{\alpha}{1-\frac{1}{3}(N/V)\alpha/\epsilon_0}\right) \tag{3.29}$$

Polarizabilities in unrationalized cgs units should be multiplied by $4\pi\epsilon_0$ for use in this formula. Using the cgs values appropriate for CS_2 ($\alpha_m = 151.4 \times 10^{-25}\,\text{cm}^3$, $\alpha = 87.6\times10^{-25}\,\text{cm}^3$, $\epsilon_L/\epsilon_0 = 2.66$ and $N/V = 10^{22}\,\text{cm}^{-3}$) we find $\delta\epsilon/\epsilon_L = 1.30$. Another parameter worth noting for CS_2 is the critical power required for threshold according to this paraxial ray theory: $P_{cr} = 2.02$ kW. This value is obtained from Eq. (3.3) for $\lambda = 6943$ Å and ϵ_2' given by the theory described in this section suitably modified by the Lorentz local-field theory. [See Eq. (6) of Ref. 19.]

IV. COUPLING OF POLARIZATIONS

For a wave of general elliptical polarization, there will be two partial differential equations describing the components of the electric field vector in each possible state of polarization. These equations will be coupled for two reasons. First, the material will, in general, couple the two components through the nonlinear susceptibility. Second, since $\nabla(\nabla\cdot\vec{E}) \neq 0$, the wave equation for one component will depend upon the other. We shall not consider this effect at all, but shall include only the coupling arising from molecular reorientation.

Close *et al.*[19] have developed the following expression for the nonlinear susceptibility tensor of the system described in the previous section:

$$\chi_{ij} = \tfrac{1}{4}\epsilon_2' \sum_{kl}(3\delta_{ik}\delta_{jl} - \delta_{ij}\delta_{kl})(E_k^* E_l + E_k E_l^*), \tag{4.1}$$

where

$$\epsilon_2' = \frac{N\beta}{90V}[(\alpha_1-\alpha_2)^2 + (\alpha_2-\alpha_3)^2 + (\alpha_3-\alpha_1)^2],$$

and the α_i are the principal molecular polarizabilities. In the limit of small field strengths, Eq. (3.26) is a special case of (4.1) for $\alpha_1 = \alpha_2 = \alpha_\perp$, $\alpha_3 = \alpha_\parallel$ and $E_i = E\delta_{i1}$.

A description in terms of Cartesian components of $\vec{E}$ is not useful here, because in this case the nonlinear polarization $\mathcal{P}_{NL}$ depends upon the relative phases of the components as well as on their magnitudes. For polarization in the x-y, plane we have

$$\mathcal{P}_{NLx} = \epsilon_2'[|E_x|^2 + \tfrac{1}{4}(3e^{2i\phi}+1)|E_y|^2]E_x \ ,$$

$$\mathcal{P}_{NLy} = \epsilon_2'[|E_y|^2 + \tfrac{1}{4}(3e^{-2i\phi}+1)|E_x|^2]E_y \ ,$$

where ϕ is the relative phase $\phi_y - \phi_x$ of the two components. Thus χ_{ij} is a function of intensities alone only when the principal axes of the polarization ellipse are aligned along the coordinate axes: $\phi = \pi/2$. However, one consequence of the coupling between the two polarizations is a rotation of the axes of the polarization ellipse, a process which requires transfer of power from one linearly polarized beam to the other. A description of the light in terms of circularly polarized components avoids this difficulty. Defining

$$\sqrt{2}\,E_\pm = E_x \pm iE_y \ ,$$

$$\sqrt{2}\,\mathcal{P}_{NL\pm} = \mathcal{P}_{NLx} \pm i\mathcal{P}_{NLy} \ ,$$

we find,

$$4\mathcal{P}_{NL\pm} = \epsilon_2'(7|E_\mp|^2 + |E_\pm|^2)E_\pm \ . \tag{4.2}$$

The two directions of rotation are coupled in a very simple way: One wave affects the dielectric constant of the other, but the dielectric constant itself can be treated as a scalar for each wave. Notice that the nonlinear susceptibility is larger for the weakest wave. Thus the weakest beam will focus more rapidly, tending to equalize the intensities of the components and convert the beam to linear polarization. Also, because the indices are different for the two components, the orientation of the ellipse rotates as the beam passes through the liquid, which is consistent with the experimental result that the beams emerge depolarized.

The saturation of a dielectric medium is inherently tensorial. Indeed, when the applied field is linearly polarized, it induces an anisotropy in the medium. The dielectric tensor describing this uniaxial medium cannot be diagonalized in the circular-polarization description and depends upon the relative

phases of the counter-rotating fields. We shall not treat the problem of the saturation of the polarizability in this section. Our discussion of saturation for linearly polairzed beams led to the conclusion that there should be periodic foci. That this is also a feature of elliptically polarized beams has been demonstrated by one of the authors (HAH) and co-workers.

Assuming, as in Sec. II, that

$$|E_{\pm}|^2 = (\mu/\epsilon_L)^{1/2}(2P_{\pm}/\pi a_{\pm}^2)\, e^{-r^2/a_{\pm}^2},$$

we may derive the following set of coupled equations for the dimensionless radii $\eta_+^* = a_+/a_0$, $\eta_-^* = a_-/a_0$ exactly as for the case of linear polarization

$$d^2\eta_+^*/d\xi^{*2} = (1-c)/\eta_+^{*3} - 7d\eta_+^*/\eta_-^{*4}, \quad (4.3)$$

$$d^2\eta_-^*/d\xi^{*2} = (1-d)/\eta_-^{*3} - 7c\eta_-^*/\eta_+^{*4}. \quad (4.4)$$

Here $4c = P_+/P_{cr}$, $4d = P_-/P_{cr}$, and we have made use of (4.2). P_+ and P_- are the powers in the counter-rotating components. These equations, of course, reduce to (2.16) with U given by (3.2) for the case of linear polarization for which $\eta_+^* = \eta_-^*$, $P_+ = P_- = \frac{1}{2}P$, $c = d = P/8P_{cr}$.

A rough idea of the behavior of the solutions of (4.3) and (4.4) may be obtained from the following crude argument. The stability analysis of Bespalov and Talanov[9] shows that the results for elliptical polarization may be obtained from those for linear polarization by diminishing the power in the latter case by the factor $\frac{1}{8}\{1+[1+(192P_+P_-/P^2)]^{1/2}\}$. [This can be obtained from the expression for $F_1(\beta)$ in Ref. 9 after replacing the quantity $(1-\beta^2)/(1+\beta^2)$ by its square to obtain the correct result.] Including this factor in Eq. (3.5) for $\dot{a}_0 = 0$, we find

$$\frac{z_f}{ka_0^2} = \left\{\frac{P}{8P_{cr}}\left[1+(1+192P_+P_-/P^2)^{1/2}\right]-1\right\}^{-1/2}.$$

Numerical analysis of Eqs. (4.3) and (4.4) indicates that this expression overestimates z_f no more than 5% for ratios of major to minor axes of the polarization ellipse of more than 3:2 at all powers, and is somewhat better for $P > 30P_{cr}$.

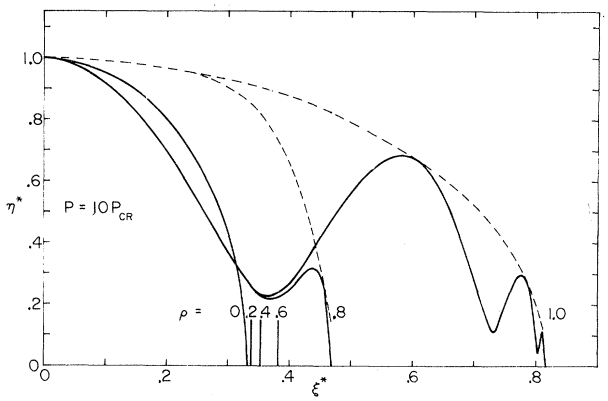

FIG. 9. Radius versus axial distance (in same variables as Fig. 1) for weaker (solid) and stronger (dashed) counter-rotating components of elliptically polarized self-focusing beams. ρ is ratio of the minor to the major axis of polarization ellipse. Only the self-focusing distance is shown for $\rho = 0.2$, 0.4, and 0.6. $P = 10P_{cr}$.

Of course Eqs. (4.3) and (4.4) are themselves approximate, and great reliance must not be placed upon these numbers. Figure 9 shows computer solutions of Eqs. (4.3) and (4.4) for several values of ρ, the ratio of minor to major axes of the polarization ellipse. For $\rho = 0.2$, 0.4, and 0.6, only the distance ξ_f^* where the radius of one of the counter-rotating components vanishes is indicated. The dashed lines are the "trajectories" of the component beam having the greater power. Notice how sensitive the self-focusing length is to small departures from circular polarization. One may expect the striking oscillations of the radius of the weaker component to be a feature of less approximate solutions of the nonlinear wave equation.

ACKNOWLEDGMENTS

We are grateful to Lloyd Huff and Richard Reynolds for assistance in numerical computations and curve plotting. One of us (JHM) is grateful to J. P. Gordon for conversations regarding this work.

*This work was partially supported by the U.S. Army Research Office, Durham, Grant No. DA-ARO-D-31-124-G920 and Joint Services Electronics Program (U.S. Army, Navy, Air Force) Grant No. AF-AF OSR-496-67.

[1]E. Garmire, R. Y. Chiao, and C. H. Townes, Phys. Rev. Letters 16, 347 (1966).

[2]P. Lallemand and N. Bloembergen, Phys. Rev. Letters 15, 1010 (1965).

[3]Y. R. Shen and Y. J. Shaham, Phys. Rev. Letters 15, 1008 (1965).

[4]G. Hauchecorne and G. Mayer, Compt. Rend. 261, 4014 (1965).

[5]G. Bret and G. Mayer, in Proceedings of the International Conference on the Physics of Quantum Electronics 1965, edited by P. L. Kelley, B. Lax, and D. E. Tannenwald (McGraw-Hill Book Co., Inc., New York, 1966), p. 180.

[6]R. Y. Chiao, E. Garmire, and C. H. Townes, Phys. Rev. Letters 13, 479 (1964).

[7]H. A. Haus, Appl. Phys. Letters 8, 128 (1966).

[8]P. L. Kelley, Phys. Rev. Letters 15, 1005 (1965).

[9]V. I. Bespalov and V. I. Talanov, Zh. Eksperim. i Teor. Fiz. – Pis'ma Redakt. 3, 471 (1966) [English transl.: JETP Letters 3, 307 (1966)].

[10]J. D. Reichert and W. G. Wagner, IEEE J. Quantum Electron. 4, 221 (1968); see also T. K. Gustafson, P. L. Kelley, R. Y. Chiao, R. G. Brewer, Appl. Phys. Letters 12, 165 (1968).

[11]V. I. Talanov, Zh. Eksperim. i Teor. Fiz. – Pis'ma Redakt. 2, 218 (1965) [English transl.: JETP Letters 2, 138 (1965)].
[12]Yu P. Raizer, Zh. Eksperim. i Teor. Fiz. – Pis'ma Redakt. 4, 3 (1966) [English transl.: JETP Letters 4, 1 (1966)].
[13]S. K. Akhmanov, A. P. Sukhorukov, and R. V. Khokhlov, Zh. Eksperim. i Teor. Fiz. 50, 1537 (1966) [English transl.: Soviet Phys. – JETP 23, 1025 (1966)].
[14]K. A. Brueckner and S. Jorna, Phys. Rev. Letters 17, 78 (1966); Phys. Rev. 164, 182 (1967).
[15]W. Kaiser, A. Laubereau, M. Maier, and J. A. Giordmaine, Phys. Letters 22, 60 (1966).
[16]Handbook of Mathematical Functions, edited by M. Abramowitz and I. A. Stegun, Natl. Bur. Stds. Appl. Math. Series 55, U. S. Government Printing Office, Washington, D. C., 1964).
[17]H. Goldstein, Classical Mechanics (Addison-Wesley Publishing Co., Reading, Mass., 1959), p. 109.
[18]R. Y. Chiao, J. D. Dodson, D. M. Irwin, and J. K. Gustafson, Bull. Am. Phys. Soc. 12, 686 (1967).
[19]D. H. Close, C. R. Giuliano, R. W. Hellwarth, L. D. Hess, F. J. McClung, and W. G. Wagner, IEEE J. Quantum Electron. 2, 553 (1966).

PHYSICAL REVIEW VOLUME 175, NUMBER 1 5 NOVEMBER 1968

Theory of Strongly Interacting Quantum Liquids. I. Formulation

W. L. McMillan*
Bell Telephone Laboratories, Murray Hill, N. J.,
and
Cavendish Laboratory, Cambridge, England
(Received 28 June 1968)

We make use of our understanding of the ground state ψ_0 and elementary excitations ψ_q of the strongly interacting Bose gas to construct a theory of strongly interacting mixed and Fermi gases. We consider the overcomplete basis set $\phi^k\psi_q$, where ϕ^k is a determinant of plane waves, and interpret the off-diagonal part of the hamiltonian as a three-point vertex, coupling the Fermi quasiparticles to the collective modes. This vertex dresses each fermion with its backflow and induces a two-fermion scattering via the interaction of the backflows. There is no residual (screened) two-body interaction in the problem. Finally we discuss the expansion parameter for strong interactions.

I. INTRODUCTION

We attempt to develop a theoretical formalism which will enable one to calculate the properties of manybody systems with strong interactions from first principles. We are interested in the case in which the dynamical correlations brought about by a strong two-body interaction dominate the correlations induced by the statistics of the particles. This is the opposite limit to the weak interactions case, i.e., the high-density electron gas[1,2] or the low-density hard-sphere Bose gas,[3,4] where the statistical correlations dominate. The physical systems that we wish to study include liquid He^3, liquid He^4, the liquid He^3-He^4 mixtures and the low-density electron gas (not the solid). The properties that we wish to calculate include the ground-state energy, the correlation functions, the elementary excitation spectrum, and the low-temperature equilibrium and transport properties.

For the weakly interacting Bose gas the kinetic energy per particle $\langle KE\rangle$ is much less than the degeneracy temperature T_B and the fraction of particles in the condensed state n_0/n is very nearly one. For the strongly interacting Bose gas we have $\langle KE\rangle \gg T_B$ and $n_0/n \ll 1$. Liquid He^4 clearly falls in the second category since, according to the microscopic theory,[5-7] $\langle KE\rangle = 14°K$, $T_B = 2.2°K$,[8] and $n_0/n = .1$. For the weakly interacting Fermi gas the kinetic energy per particle is very nearly equal to three-fifths the Fermi energy T_F and the zero-sound velocity c not much greater than the Fermi velocity v_F. For the strongly interacting Fermi gas $\langle KE\rangle \gg T_F$ and $c \gg v_F$. Liquid He^3 clearly falls in the second category since[7] $\langle KE\rangle/T_F \approx 2$ and $c/v_F = 2$.[8] We believe that it is absurd to attempt a microscopic treatment of a strongly interacting system using theoretical techniques developed for and valid only for the case of weak interactions. The purpose of this paper is to reformulate the manybody problem for strong interactions.

We will take advantage of the progress made in understanding the wave functions of the ground state and elementary excitations of liquid He^4. We will further take advantage of the fact that statistical effects are secondary so that changing bosons into fermions has only a small effect on certain properties of the system. The plan of the paper is as follows: in Sec. II we review the properties of the ground state and elementary